INTERNATIONAL JOURNAL OF CLIMATOLOGY
Int. J. Climatol. **37**: 2477–2491 (2017)
Published online 14 August 2016 in Wiley Online Library
(wileyonlinelibrary.com) DOI: 10.1002/joc.4859

RMetS
Royal Meteorological Society

Centennial drought outlook over the CONUS using NASA-NEX downscaled climate ensemble

Ali Ahmadalipour,[a]* Hamid Moradkhani[a] and Mark Svoboda[b]

[a] *Remote Sensing and Water Resources Lab, Department of Civil and Environmental Engineering, Portland State University, OR, USA*
[b] *National Drought Mitigation Center, School of Natural Resources, University of Nebraska-Lincoln, NE, USA*

ABSTRACT: Drought is a natural hazard developing slowly and affecting large areas which may have severe consequences on society and economy. Due to the effects of climate change, drought is expected to exacerbate in various regions in future. In this study, the impact of climate change on drought characteristics is assessed, and statistical methods are employed to analyse the significance of projections. This is the first study utilizing 21 recently available downscaled global climate models generated by NASA (NEX-GDDP) to evaluate drought projections over various regions across the United States. Drought is investigated through a multi-model dual-index dual-scenario approach to probabilistically analyse drought attributes while characterizing the uncertainty in future drought projections. Standardized Precipitation Index and Standardized Precipitation Evapotranspiration Index values at the seasonal scale (3 months) are used to project and analyse meteorological drought conditions from 1950 to 2099 at 0.25° spatial resolution. Two future concentration pathways of RCP4.5 and RCP8.5 are considered for this analysis. Accounting for the combined effects of precipitation and temperature variations reveals a considerable aggravation in severity and extent of future drought in the western United States and a tendency toward more frequent and intense summer droughts across the Contiguous United States.

KEY WORDS Drought; climate change; NASA-NEX; SPI; SPEI; CONUS

Received 4 April 2016; Revised 3 June 2016; Accepted 12 July 2016

1. Introduction

Drought, as a natural recurring hazard, is expected to exacerbate in various regions in the future due to the effects of climate change (Dai, 2011; Orlowsky and Seneviratne, 2013; Cook *et al.*, 2015; Zhao and Dai, 2015). It is a complex phenomenon indicating an imbalance in water availability (Madadgar and Moradkhani, 2014a; Van Loon, 2015). Several studies have assessed future changes of drought characteristics over the globe (Sheffield and Wood, 2008; Touma *et al.*, 2015), along with several regional studies of future drought conditions and impacts (Seager *et al.*, 2009; Heinrich and Gobiet, 2012; Madadgar and Moradkhani, 2013; Swain and Hayhoe, 2014; Diffenbaugh *et al.*, 2015; Duffy *et al.*, 2015; Li *et al.*, 2015; Thober *et al.*, 2015). Numerous studies have focused only on precipitation deficits due to simplicity of calculation and ease of access to the data. However, to have a better understanding of the effects of climate change on drought, it is advised to account for temperature effects as well (Strzepek *et al.*, 2010; Vicente-Serrano *et al.*, 2010; Sheffield *et al.*, 2012). Although global studies are beneficial in identifying the overall changes, studying drought at regional scales can better discern local characteristics of drought, resulting in a more accurate projection of drought conditions, which may be more useful in water resources planning and management.

The uncertainties in GCM parameterization and the existence of large biases in raw GCM outputs given the model development assumptions have resulted in overestimation of precipitation (Risley *et al.*, 2011; Sheffield *et al.*, 2013; Nasrollahi *et al.*, 2015). In a regional study over the Pacific Northwest United States, Ahmadalipour *et al.* (2015) showed that raw GCMs over-estimate summer precipitation and under-estimate winter temperature. Moreover, current GCMs have a fairly coarse resolution and therefore, are not able to reproduce small-scale regional climate characteristics (Werner, 2011; Rana and Moradkhani, 2016; Rana *et al.*, 2016). The bias corrected and downscaled GCMs provides less erroneous data and also finer scale realizations of climate scenarios improving the accuracy of projections (Ficklin *et al.*, 2016). Furthermore, in order to better assess the uncertainty of future projections, an ensemble modeling approach is recommended (Knutti, 2008). Several studies have applied objective multi-modeling methods in order to reduce the model uncertainty of future projections, and to provide likely future projections (Madadgar and Moradkhani, 2014b; Demirel and Moradkhani, 2016; Najafi and Moradkhani, 2015a, 2015b). Therefore, utilizing raw GCMs, as well as employing only a few models, are perceived as the main deficiencies in climate change impact studies, which

* Correspondence to: A. Ahmadalipour, Remote Sensing and Water Resources Lab, Department of Civil and Environmental Engineering, Portland State University, Portland, OR, USA. E-mail: aahmad2@pdx.edu

may result in biased conclusions (Rupp *et al.*, 2013; Ahmadalipour *et al.*, 2015) or may result in a poor understanding of uncertainties in drought projections.

The importance of applying appropriate indices for drought assessment is also discussed in various studies (Mishra and Singh, 2010), and several researchers have demonstrated the impacts of temperature on evapotranspiration and drought (Strzepek *et al.*, 2010; Sima *et al.*, 2013; Trenberth *et al.*, 2014; Shukla *et al.*, 2015). Different drought indices can eventuate in diverse results (Burke, 2011). The Standardized Precipitation Evapotranspiration Index (SPEI; Vicente-Serrano *et al.*, 2010), is among the fairly new indices, which is calculated based on the difference between precipitation and potential evapotranspiration (PET), thus accounting for temperature changes as well as precipitation variations. However, the Standardized Precipitation Index (SPI; McKee *et al.*, 1993) solely considers precipitation variations. Unlike some other indices with fixed temporal scale, e.g. the Palmer Drought Severity Index (PDSI;Palmer, 1965), both of these indices, i.e. SPI and SPEI, have the advantage of multi-scale application, which is essential in addressing different drought types (Vicente-Serrano *et al.*, 2010).

Given the extensive serious impacts of drought, understanding its causes in the past and projecting future drought conditions is an important task in drought studies, and has been well received in the literature. Many recent studies have employed various drought indices and have assessed trends in drought duration or severity (Dubrovský *et al.*, 2014; Park *et al.*, 2014; Yu *et al.*, 2014; Duffy *et al.*, 2015; Madhu *et al.*, 2015; Swain and Hayhoe, 2015), investigated the relationship of drought and climate teleconnections (Kam *et al.*, 2014; Huang *et al.*, 2015; Meque and Abiodun, 2015; Ujeneza and Abiodun, 2015), or evaluated the causes of a particular drought event (Griffin and Anchukaitis, 2014; Diffenbaugh *et al.*, 2015; Mao *et al.*, 2015; Seager *et al.*, 2015; Williams *et al.*, 2015; Otkin *et al.*, 2016). Improvements in accuracy and spatial resolution of datasets as well as greater availability and accessibility to ensembles of models with more realistic physical assumptions, allows for a better assessment of drought attributes in different regions while also characterizing the uncertainty of drought projections (Barnston and Lyon, 2016).

The present study aims to investigate future impacts of global warming and climate change on drought characteristics over the Contiguous United States (CONUS). This study shows the first attempt in utilizing the newly available downscaled NASA datasets (NEX-GDDP) to investigate future seasonal drought conditions over the CONUS. Three main attributes of drought are studied: spatial extent of drought (percentage of area under drought), trends in drought intensity, and changes in frequency of drought. All of these characteristics are analyzed separately for each season across different regions within the CONUS and the results are investigated for each case. Finally, the relationship between various climate variables and changes in drought attributes are studied to figure out the probable factors involved in drought worsening in the future.

2. Methods

2.1. Model selection and data

Precipitation (Prec), maximum and minimum near-surface temperature (T_{Max} and T_{Min}) from 21 statistically downscaled Global Climate Models (GCMs) were acquired on daily timescale from NASA Earth Exchange Global Daily Downscaled Projections (NEX-GDDP) (Thrasher *et al.*, 2012; dataset URL: https://nex.nasa.gov/nex/projects/1356/). All of the models are included among the GCMs archived within the Coupled Model Intercomparison Project Phase 5 (CMIP5; Taylor and Stouffer, 2012), and are statistically downscaled to $0.25° \times 0.25°$ spatial resolution. The dataset includes 21 models and a brief description about the models is provided in Table 1. The historical period of record for the dataset is from 1950 to 2005, and the future period covers years 2006 to 2099. Two representative concentration pathways (RCP4.5 and RCP8.5) are available in the dataset and were utilized in this study.

Observed precipitation from the Climate Prediction Center's (CPC) U.S. Unified Precipitation data set (Higgins and Center, 2000; $0.25° \times 0.25°$ gridded daily data, available from 1948 to 2006), and observed temperature from the University of Delaware (Willmott and Robeson, 1995'$0.5° \times 0.5°$ gridded monthly data, available from 1901 to 2010) were both acquired from the NOAA/OAR/ESRL, and used for the period of 1950–2005 (base period). Three main reasons for this selection are: (1) these datasets cover the historical period of downscaled GCMs; (2) they have a fine spatial resolution similar to that of the downscaled GCMs; and (3) they are both based on gauge-based observation. To ensure consistent spatial resolution, observed temperature data are interpolated to $0.25°$ resolution using a bilinear interpolation technique.

2.2. Drought analysis

2.2.1. Standardized Precipitation Index

SPI was developed by McKee *et al.* (1993) and is among the most prominent drought indices, widely used for drought assessment in various studies around the globe. It is based on precipitation variations and distinguishes drought by quantifying precipitation deviation from historical mean. Therefore, an SPI of zero implies that precipitation is equal to the mean of historical records. A true strength of the SPI is that it can be calculated at different timescales (e.g. 1, 3, 6, 9, 12, 24, and longer).

In this study, the SPI is calculated for a 3-month timescale in order to investigate seasonal drought attributes. To calculate the SPI, first the seasonal precipitation values for spring (AMJ), summer (JAS), fall (OND), and winter (JFM) are obtained. Then, the seasonal precipitation deficits are calculated (deviation of precipitation from historical mean), and then fitted to a gamma distribution, as proposed in previous studies (McKee *et al.*, 1993; Stagge *et al.*, 2015; Touma *et al.*, 2015). Then, the cumulative probability of the gamma distribution is transformed into a standard normal function

Table 1. 21 GCMs used in this study and their characteristics.

No.	Model	Center	Original resolution (Lat × Lon)[a]	No. of atmospheric levels	Type
1	ACCESS1-0	Commonwealth Scientific and Industrial Research Organization/Bureau of Meteorology, Australia	1.875 × 1.25	38	AO
2	BCC-CSM1-1	Beijing Climate Center, China Meteorological Administration, China	2.8 × 2.8	26	ESM
3	BNU-ESM	College of Global Change and Earth System Science, Beijing Normal University, China	2.8 × 2.8	26	ESM
4	CanESM2	Canadian Centre for Climate Modeling and Analysis, Canada	2.8 × 2.8	35	ESM
5	CCSM4	National Center for Atmospheric Research, United States	1.25 × 0.94	26	AO
6	CESM1-BGC	Community Earth System Model Contributors [National Science Foundation (NSF), DOE, and NCAR]	1.4 × 1.4	26	AO
7	CNRM-CM5	National Centre for Meteorological Research, France	1.4 × 1.4	31	AO
8	CSIRO-MK3-6-0	Commonwealth Scientific and Industrial Research Organization/Queensland Climate Change Centre of Excellence, Australia	1.8 × 1.8	18	AO
9	GFDL-CM3	NOAA/Geophysical Fluid Dynamics Laboratory, United States	2.5 × 2.0	48	AO
10	GFDL-ESM2G	NOAA/Geophysical Fluid Dynamics Laboratory, United States	2.5 × 2.0	48	ESM
11	GFDL-ESM2M	NOAA/Geophysical Fluid Dynamics Laboratory, United States	2.5 × 2.0	48	ESM
12	INMCM4	Institute for Numerical Mathematics, Russia	2 × 1.5	21	AO
13	IPSL-CM5A-LR	L'Institut Pierre-Simon Laplace, France	3.75 × 1.8	39	ChemESM
14	IPSL-CM5A-MR	L'Institut Pierre-Simon Laplace, France	2.5 × 1.25	39	ChemESM
15	MIROC-ESM	Japan Agency for Marine-Earth Science and Technology, Atmosphere and Ocean Research Institute (The University of Tokyo), and National Institute for Environmental Studies	2.8 × 2.8	80	ESM
16	MIROC-ESM-CHEM	Japan Agency for Marine-Earth Science and Technology, Atmosphere and Ocean Research Institute (The University of Tokyo), and National Institute for Environmental Studies	2.8 × 2.8	80	ChemESM
17	MIROC5	Atmosphere and Ocean Research Institute (The University of Tokyo), National Institute for Environmental Studies, and Japan Agency for Marine-Earth Science and Technology, Japan	1.4 × 1.4	40	AO
18	MPI-ESM-LR	Max Planck Institute for Meteorology, Germany	1.9 × 1.9	47	ESM
19	MPI-ESM-MR	Max Planck Institute for Meteorology, Germany	1.9 × 1.9	95	ESM
20	MRI-CGCM3	Meteorological Research Institute, Japan	1.1 × 1.1	48	AO
21	NorESM1-M	Norwegian Climate Center, Norway	2.5 × 1.9	26	ESM

[a]All GCMs used are statistically downscaled to 0.25° resolution.
AO, coupled atmospheric–ocean model; ESM, Earth system model; ChemESM, atmospheric chemistry coupled with ESM models.

(with mean = 0 and standard deviation = 1), which will be the value of the SPI. This is done separately for each grid cell and each season over the CONUS resulting in continuity between seasonal values. The parameters of the gamma distribution are calculated based on the historical data, and the same methodology is used for future drought projections. Overall, about 13 000 grid cells across the CONUS were analyzed in this study.

2.2.2. *Standardized Precipitation Evapotranspiration Index*

SPEI was introduced by Vicente-Serrano *et al.* (2010), and has been used and received considerable attention in various studies to analyze drought condition. It is based on a climatic water balance and considers the role of temperature in drought assessment. SPEI considers the difference between precipitation and evapotranspiration (P–PET) as the parameter to characterize drought. It is a standardized index that can be calculated on different timescales and does not require any specific calibration.

In this study, the accumulation period for SPEI is 3 months, the same as SPI. In order to calculate PET, Thornthwaite method (Thornthwaite, 1948) as described by Vicente-Serrano *et al.* (2010) is applied here. Previous studies have discussed that the technique chosen for calculating PET does not have serious effect on drought prediction (Mavromatis, 2007; Vicente-Serrano *et al.*, 2010; Burke, 2011; Dai, 2012). PET is calculated on a monthly timescale and is then accumulated to seasonal periods (JFM, AMJ, JAS, and OND). Therefore the deficit

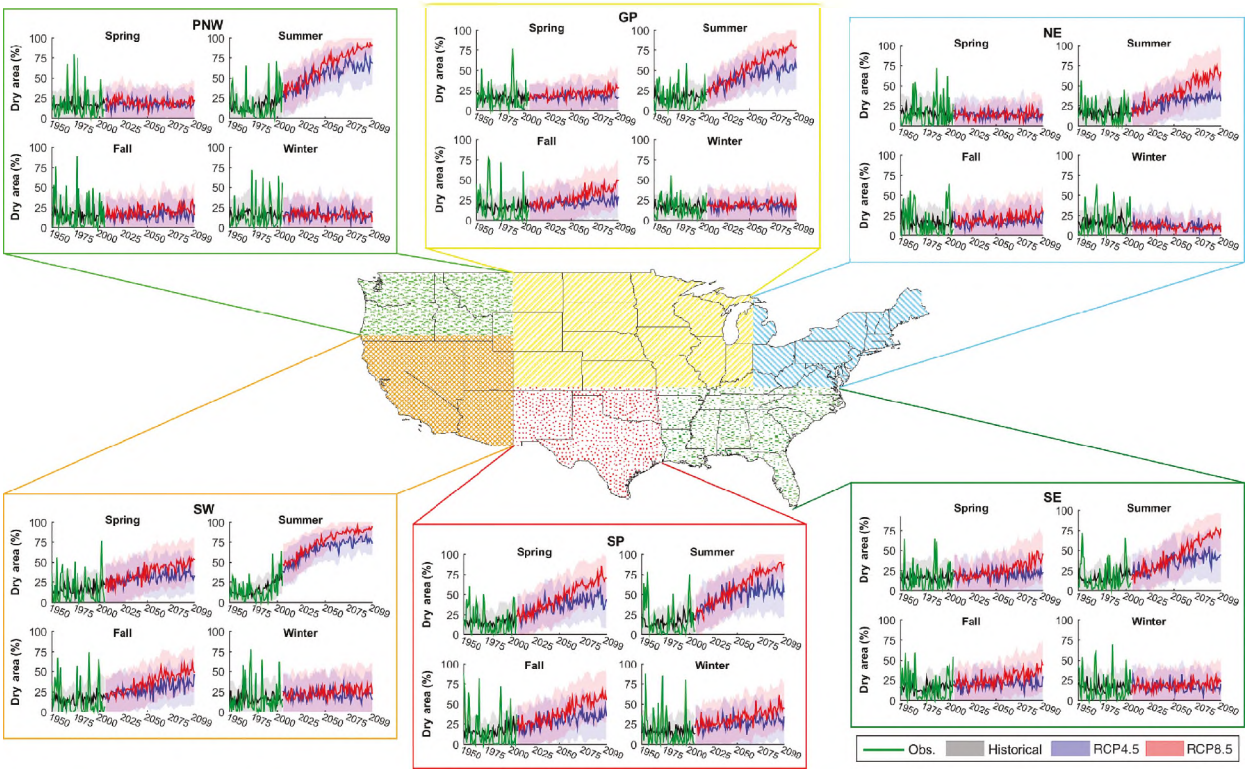

Figure 1. Spatial extent of historical and future drought across the CONUS according to the 3-month SPEI. [Colour figure can be viewed at wileyonlinelibrary.com].

(D) is calculated for each season as the difference between seasonal precipitation and seasonal PET:

$$D_3 = P_3\text{-}PET_3$$

where D_3 is the seasonal deficit of a particular season, P_3 is the seasonal precipitation, and PET_3 is the seasonal accumulated PET.

In order to calculate the SPEI, we utilized empirical Weibull plotting position (Weibull, 1939), as a nonparametric approach which would eliminate the parametric distribution selection and fitting process, as follows:

$$p\left(x_i\right) = \frac{i}{n+1}$$

where n is the sample size, i indicates the rank of P–PET data from the smallest, and $p(x_i)$ denotes the empirical probability of each time step. $p(x_i)$ is then transformed into a standardized normal distribution to obtain SPEI values. Among the various plotting positions, the Weibull function has proven to have the best performance in estimating the cumulative distribution function (CDF) by order-ranked sample (Makkonen, 2008). Applying a nonparametric method relaxes the problem of an unrestricted extrapolation, and thus very low/high SPEI values, and puts reasonable limits on the drought index (Stagge *et al.*, 2015). This helps in calculating trends of SPEI more reasonably and prevents acquiring inaccurate trends. Although nonparametric approaches might not result in the best performance for extreme droughts (Touma *et al.*, 2015), they are suitable for this study as the focus here is on moderate to extreme droughts and not only extreme droughts. The procedure was applied separately for each of the 21 GCMs in each season over the grid cells covering CONUS. Overall, approximately 13 000 grid cells across the CONUS were analyzed in this study.

2.2.3. *Drought characteristics*

For each drought index, three main characteristics of drought are studied for each season:

- Spatial extent of drought
- Intensity of drought
- Frequency of drought (number of drought events)

Spatial extent of drought was calculated for six different regions similar to those selected by Cai *et al.* (2014). The regions are shown in Figure 1, represented as Pacific Northwest (PNW), Great Plains (GP), Northeast (NE), Southwest (SW), Southern Plains (SP), and Southeast (SE). Long-term linear trends of drought intensity are investigated for 95 years of 2005–2099. Lastly, frequency of drought events are calculated for 50-year periods for the intermediate future (2006–2055), and distant future (2050–2099), and they are compared to the frequency of drought events observed during the historical period (1950–1999).

Drought indices produced for the future are calculated using the information acquired from the historical period. The base period used to calculate the drought indices is 1950–2005. For each of the 21 GCMs, the SPI and

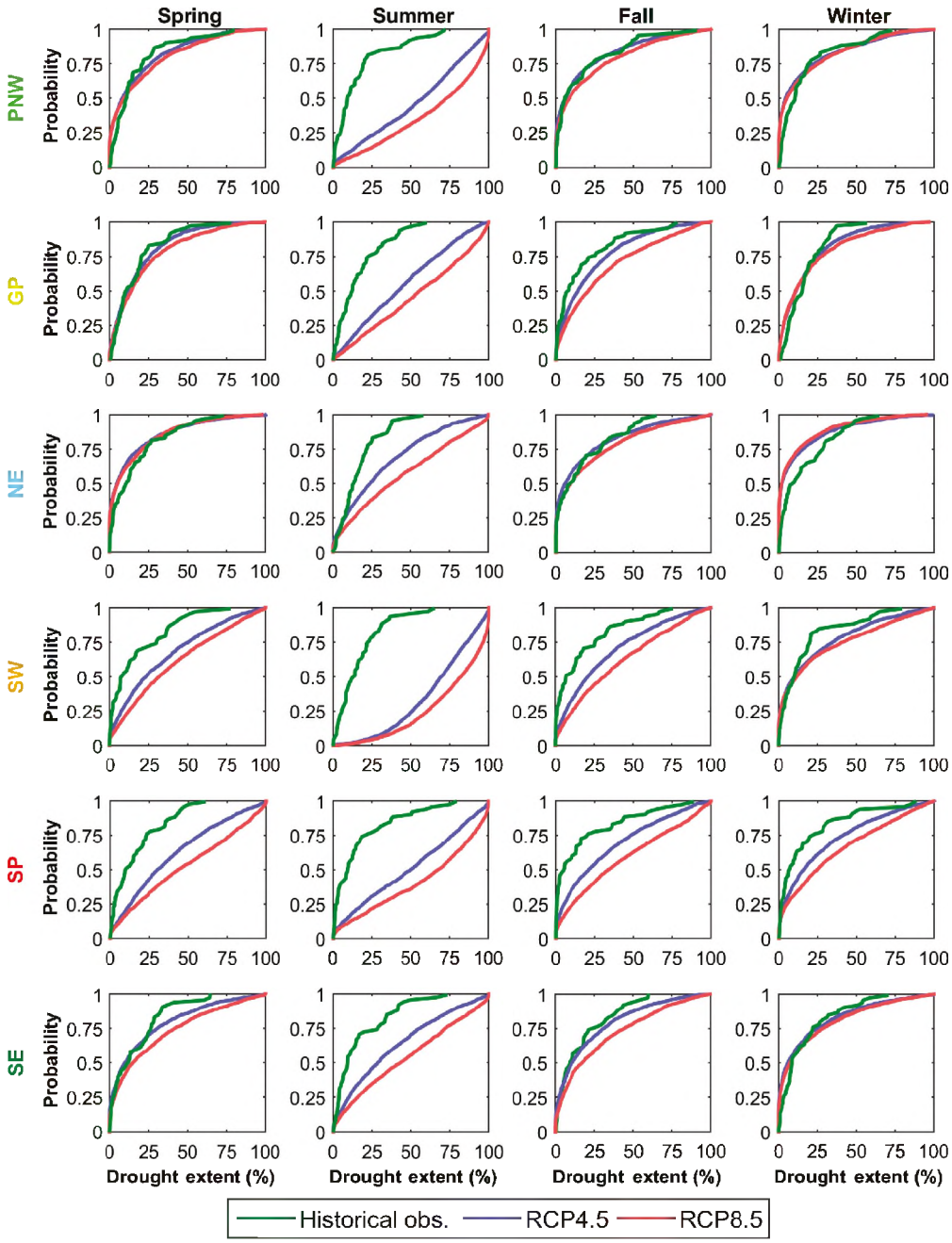

Figure 2. Probability of observed and projected drought extent based on the 3-month SPEI. [Colour figure can be viewed at wileyonlinelibrary.com].

SPEI are calculated using 3-month data (JFM, AMJ, JAS, and OND) of P and P−PET, respectively. The 3-month timescale for SPI and SPEI has shown to be the most practical timescale to study seasonal drought characteristics (Stagge *et al.*, 2015), thus it was utilized in this study. Similar to previous studies, drought onset is defined as when the index goes below -1 (moderate to extreme drought conditions; (Chen *et al.*, 2012; Heinrich and Gobiet, 2012).

2.3. Kolmogorov–Smirnov test

The Kolmogorov–Smirnov (KS) test is one of the most commonly used and applicable nonparametric methods for comparing two samples to understand whether they come from populations with the same distribution. The test is based on the distance between the two empirical distributions and is sensitive to differences in both location and shape of probability functions. The null hypothesis is that the two distribution functions have the same distribution. The P-value calculated from the test will be compared to a certain significance level (in this study, $\alpha = 0.05$), and if it is lower than α, the null hypothesis is rejected and thus the two CDFs are not from the same distribution. In this study, the KS test is used to quantify if the changes in likelihood of drought extent in the future are significantly different from that of historical observations.

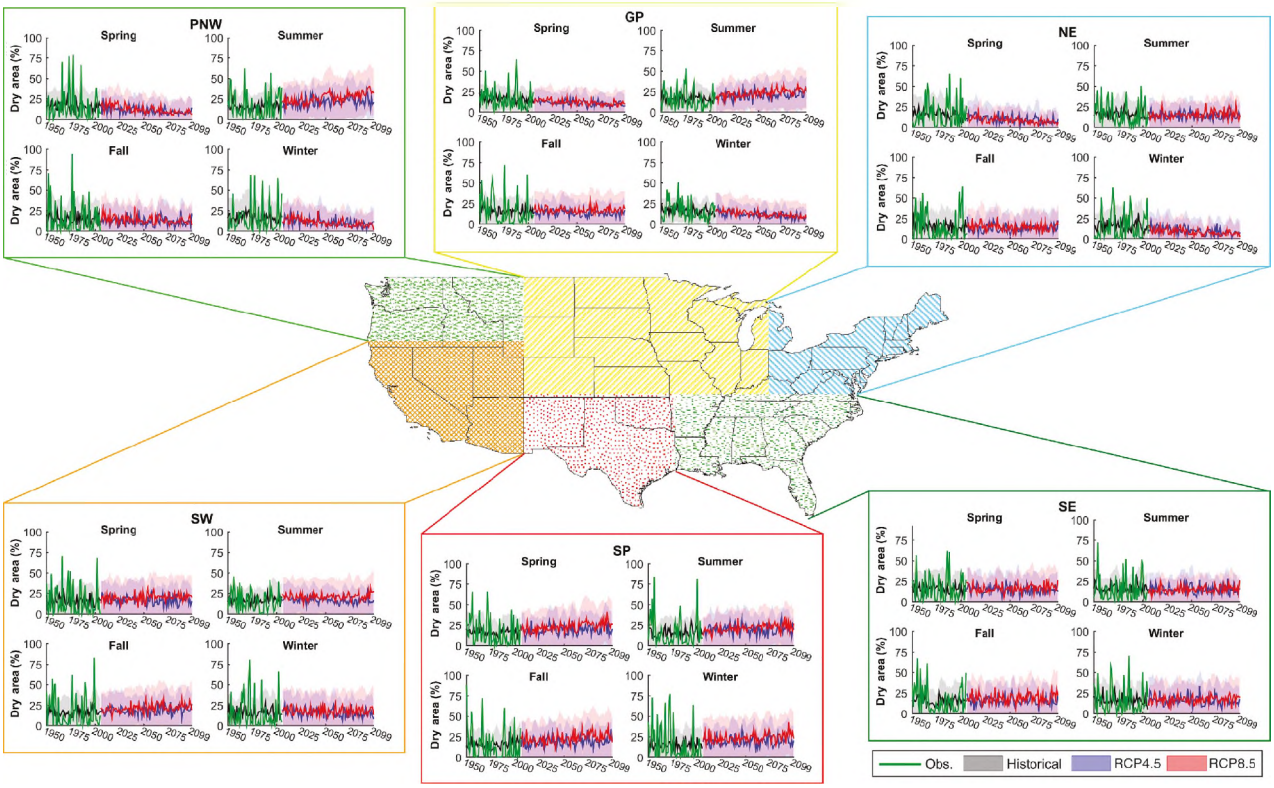

Figure 3. Spatial extent of historical and future drought according to the 3-month SPI. [Colour figure can be viewed at wileyonlinelibrary.com].

3. Results

3.1. Spatial extent of drought

Figure 1 shows the spatial extent of drought according to the SPEI index in six different regions across the CONUS for the period of 1950–2099. For each year, the spatial extent of drought (percentage of area with SPEI below −1) is calculated for 21 downscaled GCMs and then the mean and ±1 standard deviation of the results are plotted for each case. As seen in this figure, the GCM ensemble spread envelopes most of the variations in observed drought extent. The patterns are characterized by a vast increase in drought extent for summer in all regions, especially in the western United States and Southern Plains. Predictions of summer drought extent for the SW show the most increase in drought extent in distant future while also having the lowest uncertainty compared to the other regions. The increase in drought extent over the historical period is noticeable for summer observations (green line) in the SW and PNW, and the GCM ensemble mean (black line) shows a close agreement with the observations. However, drought extent in winter shows a slightly decreasing trend in northern United States, particularly in the NE region. RCP4.5 and 8.5 suggest similar results until around 2040, with consistently larger drought extent projected by RCP8.5 after that.

Overall, the models show good agreement between the long-term mean and spatial characteristics of drought found in the historical period. Model uncertainty appears to be the primary source of uncertainty in drought projections for the near future, and only in mid to distant future summers (after 2050) scenario uncertainty becomes noticeable.

To better understand the changes in the spatial extent of drought, the probability of SPEI drought extents are plotted in Figure 2 using the empirical CDF. Future probabilities are plotted using the results of all 21 downscaled GCMs for the period 2006–2099. Probabilities are calculated using the Kaplan-Meier method as a non-parametric technique to estimate the CDF. The empirical CDF of all 21 model outputs are presented for each season and region, and thus, the change in distribution of drought extent becomes noticeable. The shift to the right in CDFs for future drought extent explains the increasing drought extent of future at the same non-exceedance probability. For instance, historical drought extent during the summer season indicates a median of less than 15% for most regions; while the projections show the median of future drought extent is expected to be above 50%. The change of probability is more significant in summers for the SW region; the median of historical drought extent is 12%, while the median of future drought extent for RCP4.5 and RCP8.5 increases to 69 and 82%, respectively. However, the NE region appears to have the least amount of change in drought extent. In some regions, the increase in drought extent is expected at higher probabilities. This indicates that even though the median of drought extent is not changing in some regions/seasons, drought would become more extensive during extreme conditions.

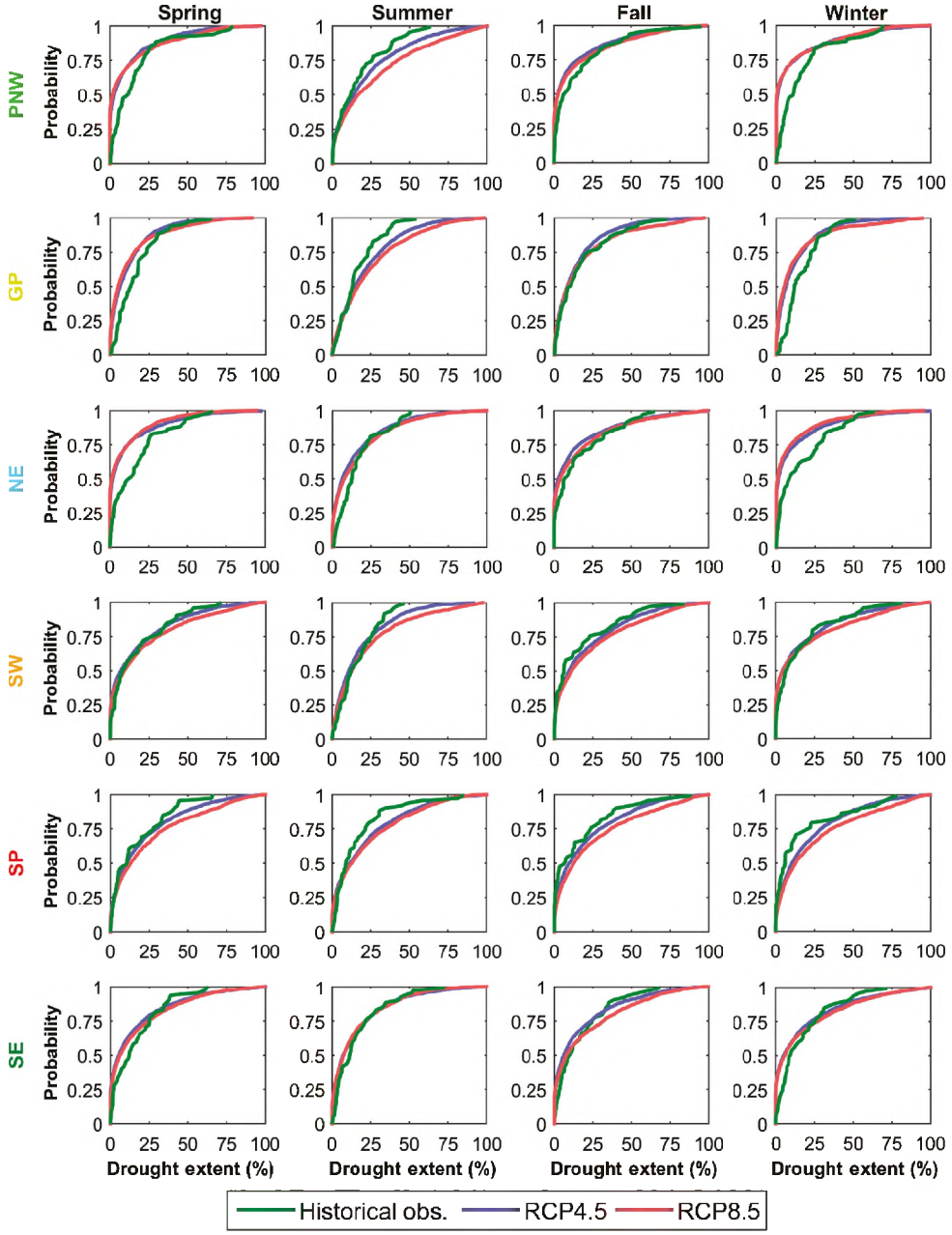

Figure 4. Probability of observed and projected drought extent based on the 3-month SPI. [Colour figure can be viewed at wileyonlinelibrary.com].

Similar results for drought extent depicted by the SPI are presented in Figures 3 and 4. Comparing drought extent calculated by SPEI and SPI reveals the effect of temperature increases. A major increase in SPI drought extent (presented in Figure 3) is found during summers in the PNW and GP, and for all seasons in SP. Similar to the SPEI, winters in the northern regions of the CONUS indicate a decrease in SPI drought extent in both future scenarios.

To better understand the changes in drought extent, a two-sample KS test was utilized to analyze the difference between the probability of drought in the future and that of the historical observation at a 0.05 significance level (95% confidence). Results of the KS test are shown in Figure 5. The KS test for the SPEI indicates significant difference (increase) between the probability of future and historical drought in all seasons for the SW and SP. The test is unable to detect any significant difference between historical and future drought extent in the spring and fall across the GP and SE, but it shows a considerable decrease in drought extent during the spring and winter in the NE. However, KS test results for the SPI are unable to detect any significant differences across the SW and SP, while indicating lower drought occurrences in most seasons across the PNW.

3.2. Trends of future drought intensity

In addition to the spatial extent of drought, it is of high importance to estimate the changes in the intensity of

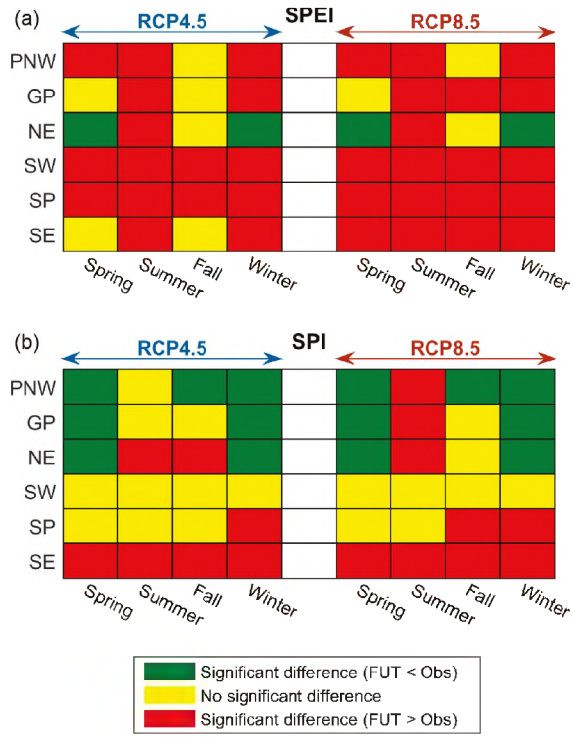

Figure 5. Comparing future and historical drought extents according to the Kolmogorov–Smirnov (KS) test. The figure is generated using data from 21 GCMs in each region. [Colour figure can be viewed at wileyonlinelibrary.com].

future droughts. Figure 6 shows the regions with a negative trend (increasing drought intensity) in the future according to the SPEI. RCP4.5 results are shown in the left column followed by RCP8.5 results on the right. To have a better understanding of drying trends, only negative trends (intensifying drought condition) are shown. In order to find trends, the SPEI is calculated for each of the 21 GCMs and the average trend from all downscaled GCMs is calculated for each grid cell. The mean change of SPEI per year for the period of 2005–2099 is then plotted. For example, a trend of −0.02 in SPEI means that in 25 years (near future), the average value of SPEI will decrease by 0.5 (-0.02×25) and also in 75 years (distant future), the average value of SPEI will decrease by 1.5 (-0.02×75), which is significant given the SPEI thresholds of −1, −1.5, and −2 representing moderate, severe, and extreme drought condition, respectively. Thus, a decrease of 0.5 in the SPEI value will worsen the severity category of a drought event by one class.

Trends are showing conforming results with drought extent, with significant changes found in summer for most regions. The concentration pathways of RCP8.5 and RCP4.5 show similar spatial patterns with more severe drought according to RCP8.5. For summer, a negative trend is estimated for the entire CONUS in both concentration pathways. This simply implies that summer droughts are expected to become more intense across the CONUS. Moreover, southern California, Arizona, and Texas show critical conditions where a decreasing trend is found in intensity of drought for all seasons.

The SPI trend results are presented in Figure 7. Similar to Figure 6, only regions with negative SPI trends (increasing drought intensity) are shown to have a better understanding about drying patterns. The RCP4.5 and RCP8.5 trend results of SPI show similar patterns with exacerbated trends depicted in the latter. Comparing trend results from the SPEI (Figure 6) and SPI (Figure 7), similar spatial patterns are found in spring and winter, with larger trends being calculated by the SPEI. In summer and fall, the SPI shows a negative trend in the northern and southern regions of the CONUS respectively, while for the SPEI, a negative trend is found almost over the entire CONUS.

3.3. Drought frequency

Another useful measure to better understand the impact of climate change on drought is to study the changes in frequency of future droughts. To obtain this, the number of drought events in 50-year periods of future projections is compared to the number of events in the historical period. Therefore, future drought projections for each of the 21 GCMs is considered, and the number of drought events (drought index < -1) is extracted for each case. Then, the average of drought events from 21 GCMs is compared to the number of historical drought events and the spatial change is plotted over 50-year time frame. This is carried out separately for each grid cell and each season. Results for the SPEI are presented in Figure 8. Increase in frequency of drought is perceived for all seasons, especially for summer. Results are in accordance with trends (presented in Figure 6), and show that Texas, Arizona, and southern California may expect a substantial increase in the frequency of drought in all seasons, while little change is found in frequency at the eastern regions.

Similar to what was applied for the SPEI, increase in the number of projected SPI drought events is presented in Figure 9. Drought frequency results from the SPI show very similar patterns to those generated by the SPEI (Figure 8), with the SPI indicating less change. For both indices, results of the RCP4.5 and RCP8.5 are very similar for the period 2006–2055. However, in the distant future (2050–2099), the RCP8.5 shows more frequent droughts than those of RCP4.5 with similar regional patterns depicted by both.

4. Discussion

Concurrent increase/decrease of future temperature/precipitation while experiencing alterations in seasonality of climatic variables makes it difficult to determine the regional characteristics of future drought conditions. Therefore, questions may arise about the role of related climate variables in drought attributes for each region.

Comparisons between the SPEI and SPI results demonstrate the paramount importance of temperature in aggravating future drought conditions. The SPI indicates a mild increase in drought extent for summers in most regions, with little discrepancy between the two future scenarios. It also shows a reduction of drought extent in spring and

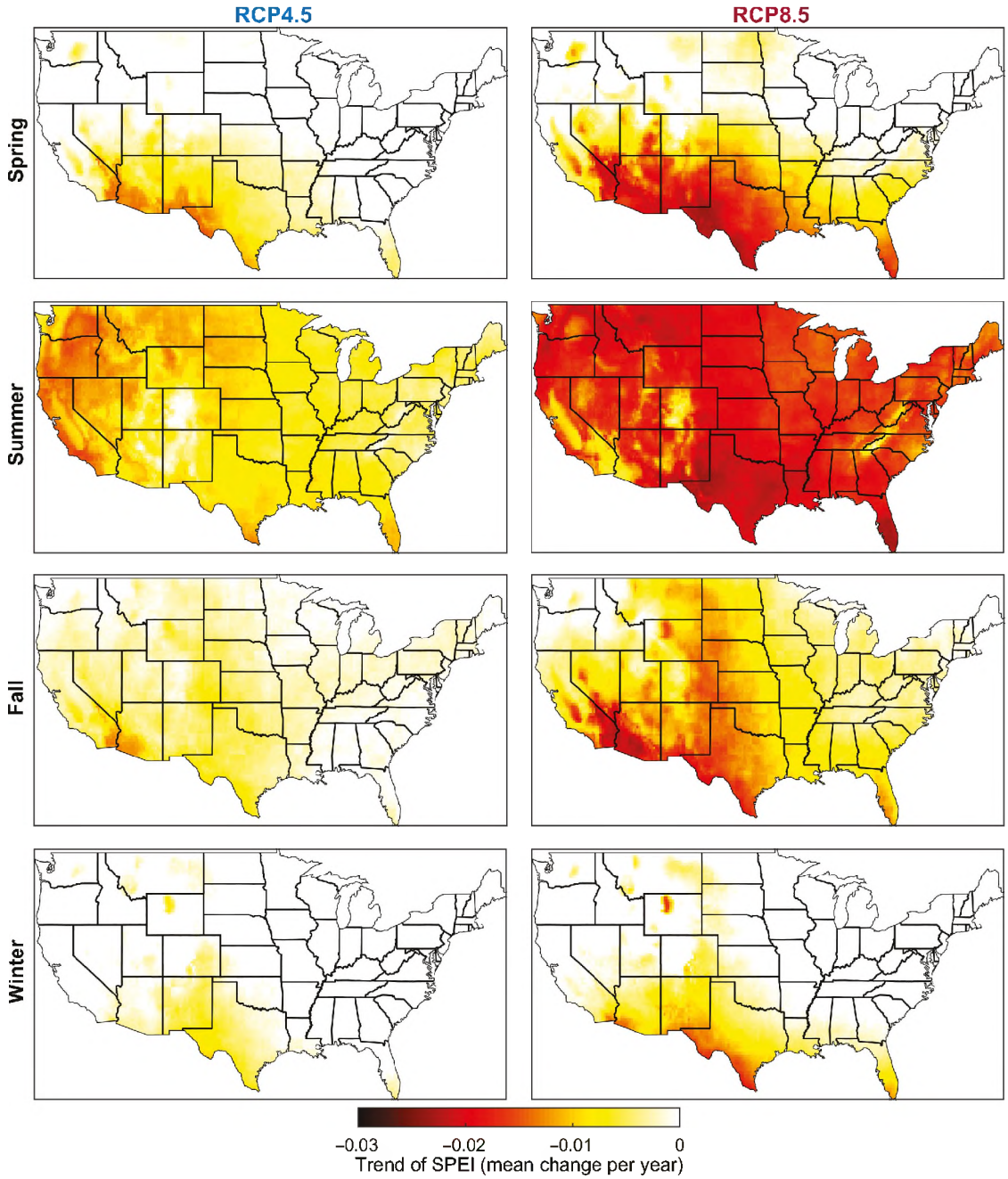

Figure 6. Long-term drought trends for the period of 2005 to 2099 according to the 3-month SPEI. Please note that a trend of −0.02 in SPEI means that in 25 years, the mean value of SPEI will decrease by 0.5 (−0.02 × 25), which is significant given the SPEI thresholds of −1, −1.5, and −2, which represent moderate, severe, and extreme drought conditions, respectively. [Colour figure can be viewed at wileyonlinelibrary.com].

winter for all northern regions. The difference between the SPI and SPEI is more considerable in the warm seasons, as in winter both indices similarly demonstrate a decrease in spatial extent of drought for northern regions (PNW, GP and NE). Furthermore, the change in intensity and increase in frequency of SPI drought events are found to be less than those of SPEI results. Using the SPI, no changes are expected for summer droughts in the SW region, while according to the SPEI, this region is expected to experience the most aggravated drought condition in the CONUS.

The SPEI calculation is based on both precipitation (Prec) and PET, and changes in each of these variables may result in changes of the SPEI. Moreover, temperature (T) is the primary variable used in calculating PET. Thus, it can be expected that the changes in Prec and PET directly affect the SPEI, while the changes in temperature may affect SPEI indirectly. Although results of the SPEI show a drastic escalation in future drought conditions, it is not clear if either the decrease in precipitation amount, change in seasonality of precipitation, or the increase in PET is the primary cause of drought

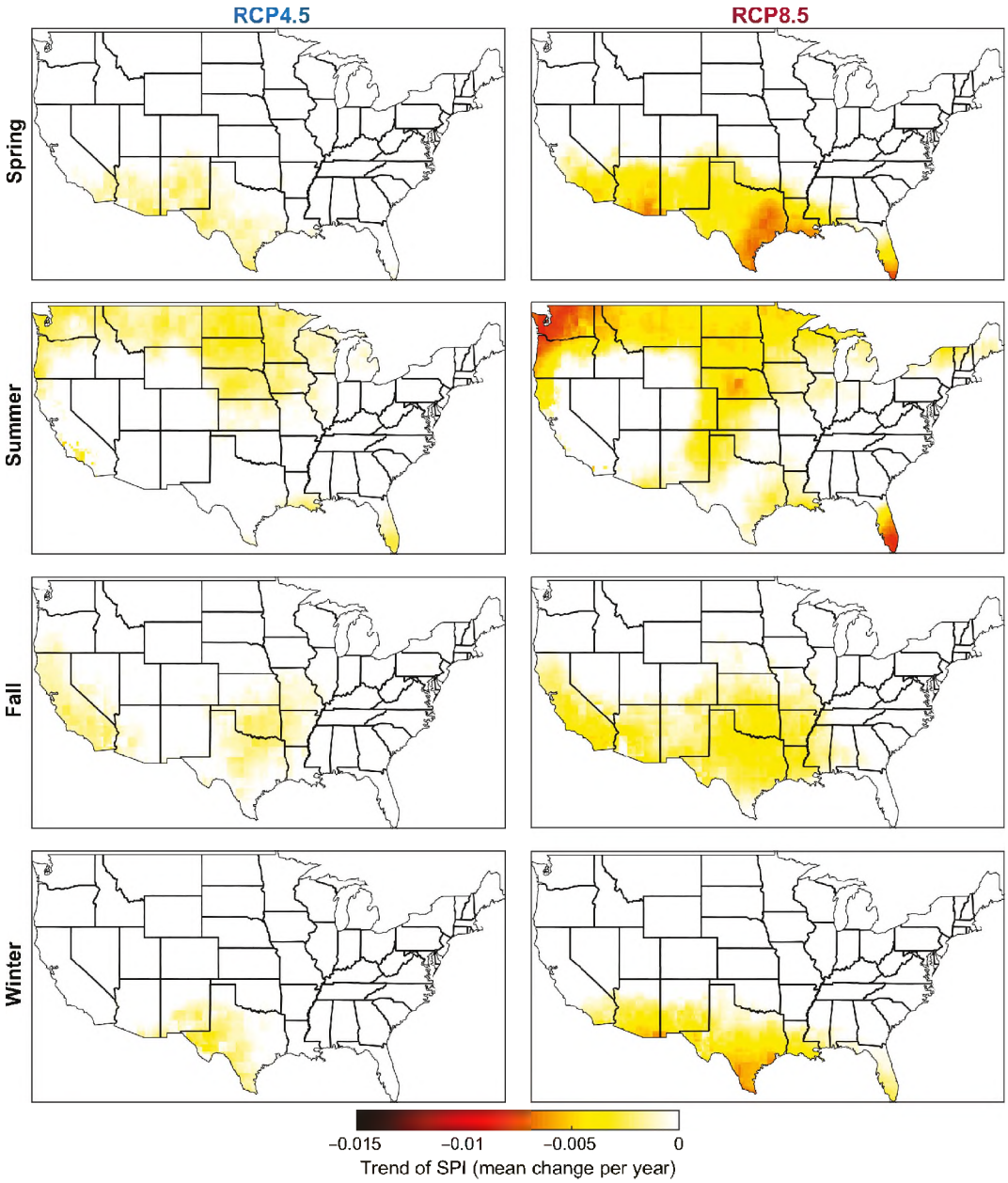

Figure 7. Long-term drought trends for the period of 2005–2099 according to the 3-month SPI. [Colour figure can be viewed at wileyonlinelibrary.com].

exacerbation. Since different regions have different climates and aridity conditions, the primary cause may differ from location to location. Therefore, studying the effects and relationship of climate variables with drought at the regional scale is of great importance. Studying the impact of changes in seasonality of precipitation and temperature on drought is out of the scope of this study. However, this may be among the main causes for aggravation of drought, and a comprehensive assessment is needed on this subject.

In order to understand the cause for changes in future drought characteristics, seasonal changes of temperature, precipitation, and PET from 21 GCMs are extracted for each season in 50-year periods for the future (2006–2055 and 2050–2099), and the ensemble mean of changes are plotted in supplementary Figures S1–S3, Supporting information. Temperature is expected to increase across the CONUS, especially in the western regions. The spring season appears to have the least increase in temperature among all seasons, and for other seasons the changes appear to be similar. In addition, precipitation shows a significant decrease during summer for the western regions and Southern Plains (more than 50% decrease in some areas), and a decrease for the central regions in fall and winter. PET is also showing considerable increase in future summers with a slight increase in fall noted as well.

To find out how the changes of each variable are related to changes in drought, a spatial correlation analysis is

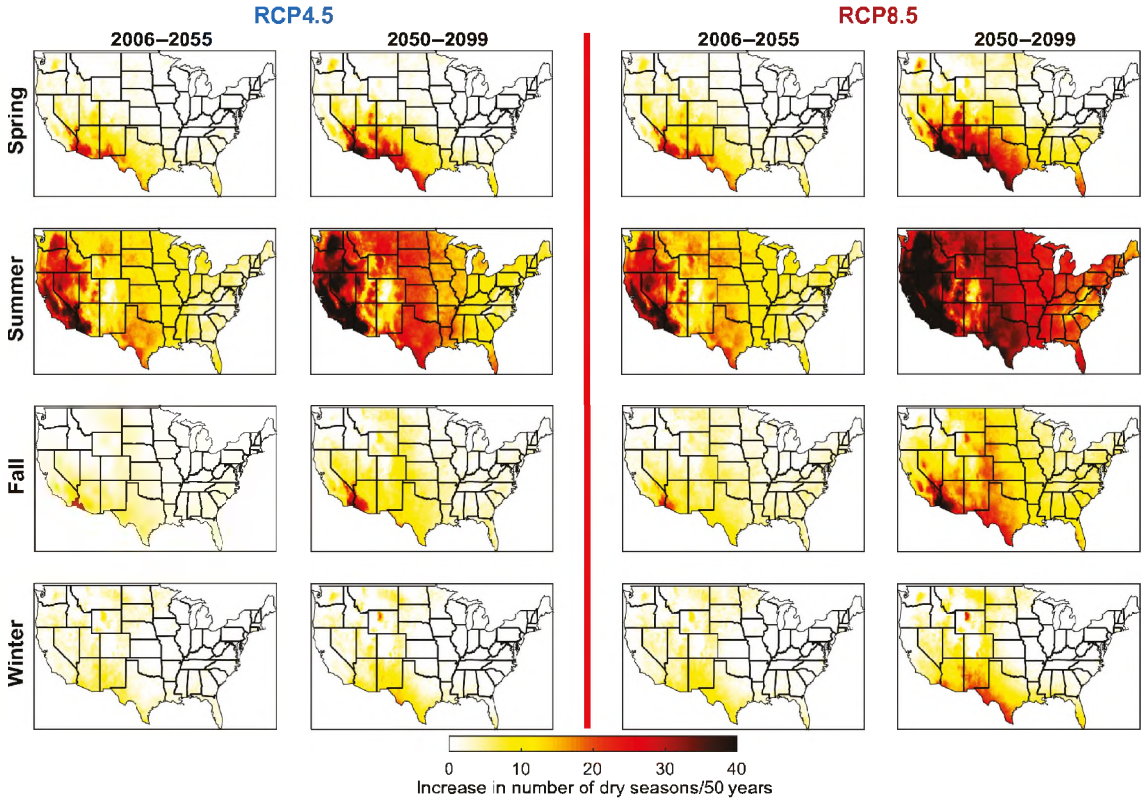

Figure 8. Increase in the number of moderate or worse drought events according to the 3-month SPEI. [Colour figure can be viewed at wileyonlinelibrary.com].

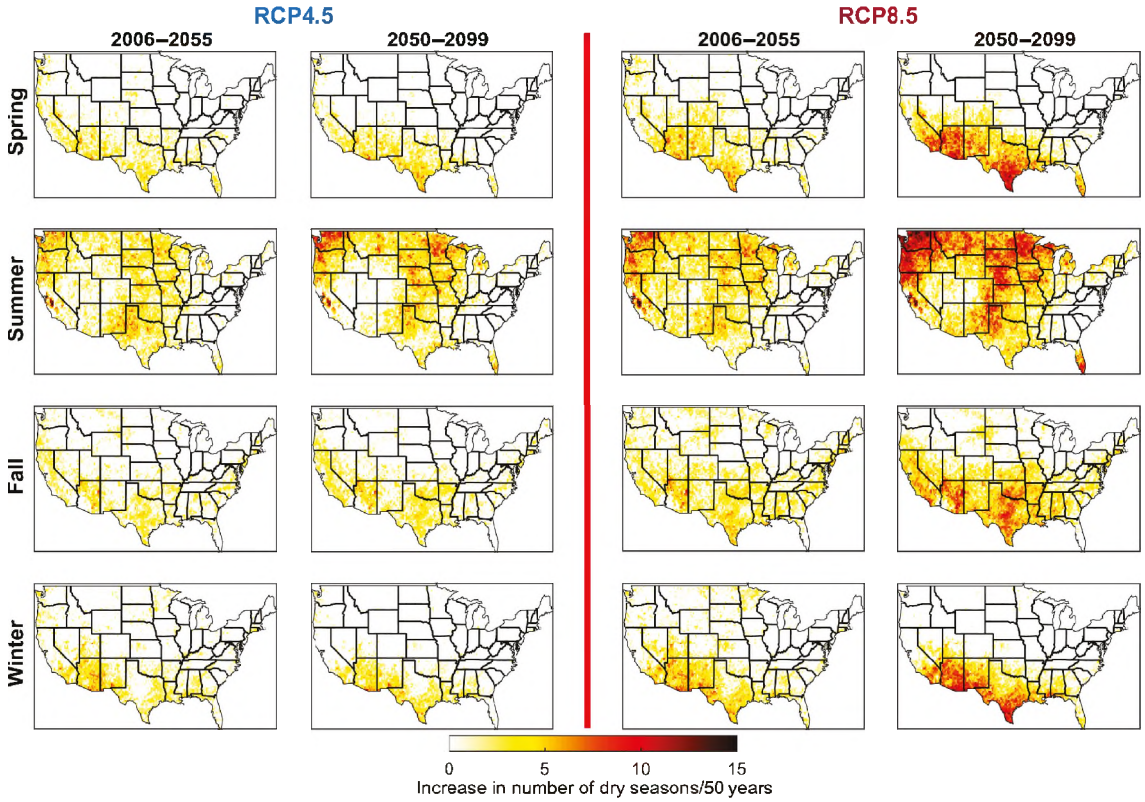

Figure 9. Increase in the number of moderate or worse drought events according to the 3-month SPI. [Colour figure can be viewed at wileyonlinelibrary.com].

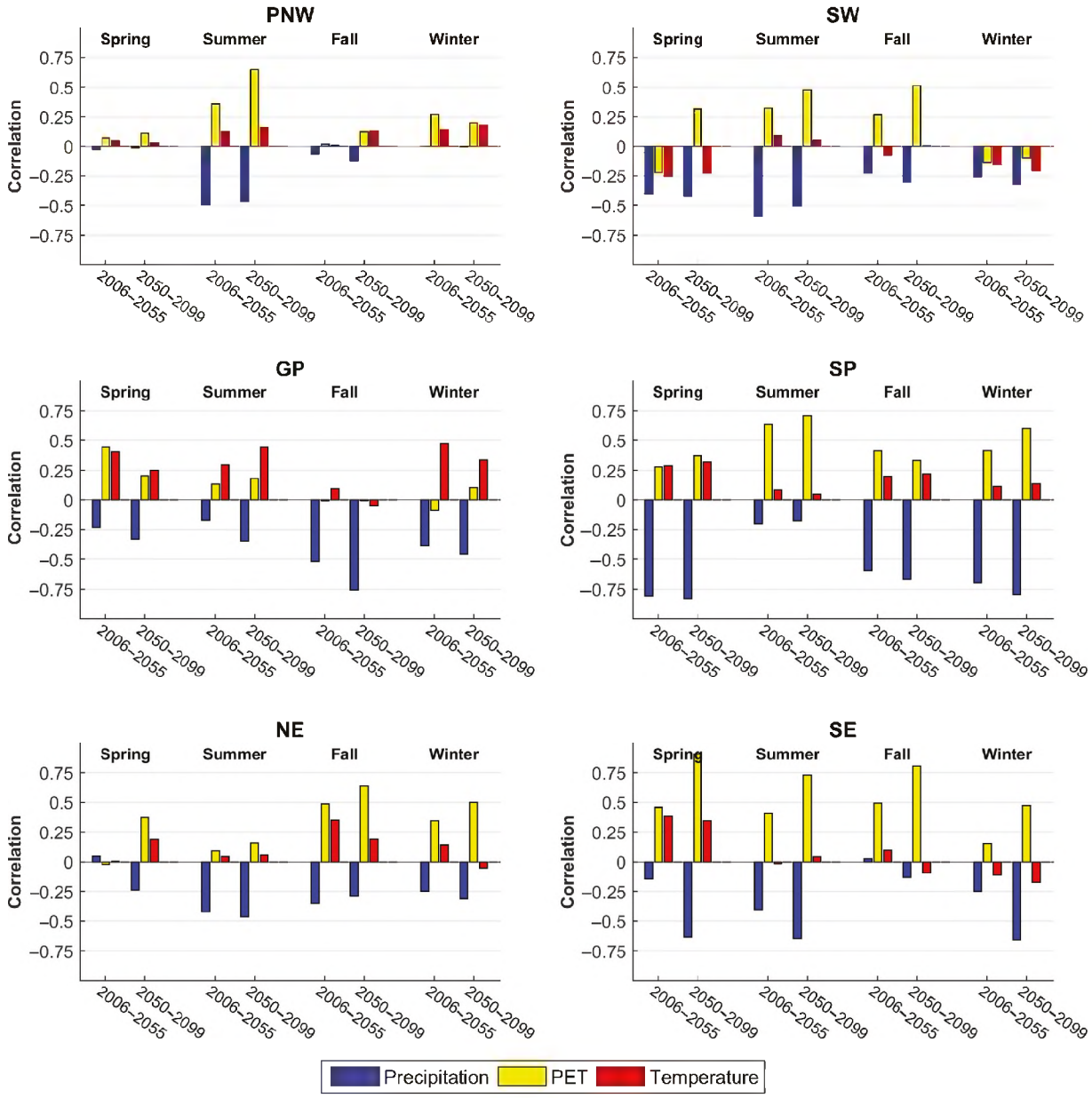

Figure 10. Spatial correlation between the changes in the number of SPEI drought events (presented in Figure 8) and the changes in climate variables (presented in Figures S1–S3) for 50-year future periods using the RCP8.5 scenario. [Colour figure can be viewed at wileyonlinelibrary.com].

applied using Spearman correlation test for each season. Figure 10 represents the spatial correlation between the increase in drought frequency (Figure 8) and the changes in each variable (Figures S1–S3) for RCP8.5. To generate Figure 10, first the increase/decrease in number of dry seasons is calculated for each grid cell (shown in Figure 8). Then, the changes in climate variables, i.e. Prec, PET, and T, are calculated for each grid (shown in Figures S1–S3). Therefore, for a region with n grid cells, one may calculate n values for the changes in number of dry seasons as well as n values for the changes in PET (Figures 8 and S3). We then calculate the correlation of these results for the n corresponding grids. In other words, Figure 10 is the spatial correlation of change in number of dry seasons and the change in climate variable. It is simply trying to find a spatial coherence between results of Figures 8 and S1–S3, to find a probable cause for changes in drought in a particular region and season. In general, one would expect that changes in precipitation negatively correlate with the changes of drought, i.e. decreasing precipitation increases drought events, and changes in PET would positively correlate with drought, i.e. increasing PET increases drought events. Our results show this to be true in most cases with high correlation.

From Figure 10, different results are found when assessing such a spatial correlation for various regions. For instance, in the Southern Plains, changes in precipitation are highly correlated with changes in drought events for all seasons except summer when changes in PET are positively correlated. Therefore, precipitation changes

(amount/seasonality) play a major role in droughts within the SP region for most of the seasons, and increases in PET has a major influence on summer droughts. On the other hand, in the PNW no significant spatial correlation can be found for spring, fall, and winter; however, summer shows a noticeable correlation between drought events and precipitation along with PET. This is also in accordance with the spatial extent of drought presented in Figure 1, where only summers exhibit a substantial increase and other seasons do not show any considerable changes. Although most regions show a high correlation amount for PET in summers, the NE and GP regions do not indicate any significant spatial correlation between drought events and PET, and changes in precipitation appears to be the primary cause for summer drought changes in these regions. In general, and in most cases, distant future (2050–2099) results show higher correlation than those in the intermediate future (2006–2055).

Results from the spatial correlation analysis of the RCP4.5 are presented in supplementary Figure S4. When comparing the RCP4.5 and RCP8.5, the patterns are similar in most cases, although in general the RCP4.5 shows a lower correlation than the RCP8.5.

5. Summary and conclusion

This study investigated meteorological drought projections over the CONUS using fine resolution downscaled CMIP5 GCMs. The dataset has recently become available by NASA (NEX-GDDP) consisting of an ensemble of daily precipitation, and maximum and minimum temperature for 21 GCMs. All 21 available models were utilized for the period of 1950–2099 for two future concentration pathways, i.e. RCP4.5 and RCP8.5. Different spatiotemporal characteristics of drought were analyzed using the SPEI and SPI utilizing seasonal accumulation periods (3-month timescale).

Results show that the spatial extent and intensity of meteorological drought is expected to increase for all regions of the CONUS in summer, primarily due to an increase in PET. Furthermore, considerable aggravation in drought attributes is projected over the Southwestern United States and Southern Plains, mainly due to changes in precipitation. The Northeastern regions of the United States show lessening drought conditions for spring and winter, while exacerbating conditions are expected during the summer due to changes in precipitation. There are large differences between the results of the SPI and SPEI with temperature changes having a substantial impact on drought characteristics, especially in the summer. Therefore, studying meteorological drought using the SPI is found to be inadequate for understanding the impacts of climate change and it is highly recommended to consider the effect of temperature in drought assessment through the use of the SPEI.

Climate change is going to impose considerable impacts on meteorological drought attributes in the future. In this study, spatial extent, intensity trends, and frequency of droughts were investigated. However, understanding the changes in duration, severity, magnitude and the onset of future droughts is also of high importance requiring further research. In addition to the seasonal drought assessment done in this study, it is useful and informative to stakeholders to characterize drought projections at different timescales to better understand regional impacts of global warming and climate change on various types of drought.

Acknowledgements

We are thankful for the financial support provided by NOAA-MAPP program, grant NA140AR4310234. Climate scenarios used were from the NEX-GDDP dataset, prepared by the Climate Analytics Group and NASA Ames Research Center using the NASA Earth Exchange, and distributed by the NASA Center for Climate Simulation (NCCS).

Supporting information

The following supporting information is available as part of the online article:

Figure S1. Projected increases in temperature in degrees celsius. Calculations are performed for each of the 21 GCMs and the mean changes are plotted here.

Figure S2. Percentage change in future precipitation projections. Changes are found for each of the 21 GCMs and the mean change is plotted here.

Figure S3. Change in future projections (in mm) of potential evapotranspiration (PET). Similar to Figures S1 and S2, changes are calculated for each of the 21 GCMs with the mean change being plotted here.

Figure S4. Spatial correlation between changes in the number of moderate or worse 3-month SPEI drought events (presented in Figure 8) and changes in climate variables (presented in Figures S1–S3) for 50-year future time periods using the RCP4.5.

References

Ahmadalipour A, Rana A, Moradkhani H, Sharma A. 2015. Multi-criteria evaluation of CMIP5 GCMs for climate change impact analysis. *Theor. Appl. Climatol.*, doi: 10.1007/s00704-015-1695-4.

Barnston AG, Lyon B. 2016. Does the NMME capture a recent decadal shift toward increasing drought occurrence in the southwestern United States? *J. Clim.* **29**(2): 561–581.

Burke EJ. 2011. Understanding the sensitivity of different drought metrics to the drivers of drought under increased atmospheric CO_2. *J. Hydrometeorol.* **12**: 1378–1394, doi: 10.1175/2011JHM1386.1.

Cai X, Yang Z-L, Xia Y, Huang M, Wei H, Leung LR, Ek MB. 2014. Assessment of simulated water balance from Noah, Noah-MP, CLM, and VIC over CONUS using the NLDAS test bed. *J. Geophys. Res. Atmos.* **119**: 13751–13770, doi: 10.1002/2014JD022113.

Chen G, Tian H, Zhang C, Liu M, Ren W, Zhu W, Chappelka AH, Prior SA, Lockaby GB. 2012. Drought in the Southern United States over the 20th century: variability and its impacts on terrestrial ecosystem productivity and carbon storage. *Clim. Change* **114**(2): 379–397, doi: 10.1007/s10584-012-0410-z.

Cook BI, Ault TR, Smerdon JE. 2015. Unprecedented 21st century drought risk in the American Southwest and Central Plains. *Sci. Adv.* **1**: 1–7, doi: 10.1126/sciadv.1400082.

Dai A. 2011. Drought under global warming: a review. *Wiley Interdiscip. Rev. Clim. Change* **2**(1): 45–65.
Dai A. 2012. Increasing drought under global warming in observations and models. *Nat. Clim. Change* **3**(1): 52–58, doi: 10.1038/nclimate1633.
Demirel MC, Moradkhani H. 2016. Assessing the impact of CMIP5 climate multi-modeling on estimating the precipitation seasonality and timing. *Clim. Change* **135**(2): 357–372.
Diffenbaugh NS, Swain DL, Touma D. 2015. Anthropogenic warming has increased drought risk in California. *Proc. Natl. Acad. Sci. U.S.A.* **112**(13): 201422385, doi: 10.1073/pnas.1422385112.
Dubrovský M, Hayes M, Duce P, Trnka M, Svoboda M, Zara P. 2014. Multi-GCM projections of future drought and climate variability indicators for the Mediterranean region. *Reg. Environ. Change* **14**(5): 1907–1919.
Duffy PB, Brando P, Asner GP, Field CB. 2015. Projections of future meteorological drought and wet periods in the Amazon. *Proc. Natl. Acad. Sci. U.S.A.* **112**(43): 201421010, doi: 10.1073/pnas.1421010112.
Ficklin DL, Abatzoglou JT, Robeson SM, Dufficy A. 2016. The influence of climate model biases on projections of aridity and drought. *J. Clim.* **29**(4): 1269–1285.
Griffin D, Anchukaitis KJ. 2014. How unusual is the 2012-2014 California drought? *Geophys. Res. Lett.* **41**(24): 9017–9023, doi: 10.1002/2014GL062433.
Heinrich G, Gobiet A. 2012. The future of dry and wet spells in Europe: a comprehensive study based on the ENSEMBLES regional climate models. *Int. J. Climatol.* **32**(13): 1951–1970, doi: 10.1002/joc.2421.
Higgins RW, Center CP. 2000. *Improved United States Precipitation Quality Control System and Analysis*. NOAA, National Weather Service, National Centers for Environmental Prediction, Climate Prediction Center.
Huang S, Huang Q, Chang J, Leng G. 2015. Linkages between hydrological drought, climate indices and human activities: a case study in the Columbia River basin. *Int. J. Climatol.* **36**(1): 280–290, doi: 10.1002/joc.4344.
Kam J, Sheffield J, Wood EF. 2014. Changes in drought risk over the contiguous United States (1901–2012): the influence of the Pacific and Atlantic Oceans. *Geophys. Res. Lett.* **41**(16): 5897–5903.
Knutti R. 2008. Should we believe model predictions of future climate change? *Philos. Trans. A Math. Phys. Eng. Sci.* **366**(1885): 4647–4664, doi: 10.1098/rsta.2008.0169.
Li X, Zhou W, Chen YD. 2015. Assessment of regional drought trend and risk over China: a drought climate division perspective. *J. Clim.* **28**(18): 7025–7037, doi: 10.1175/JCLI-D-14-00403.1.
Madadgar S, Moradkhani H. 2013. A Bayesian framework for probabilistic seasonal drought forecasting. *J. Hydrometeorol.* **14**(6): 1685–1705, doi: 10.1175/JHM-D-13-010.1.
Madadgar S, Moradkhani H. 2014a. Spatio-temporal drought forecasting within Bayesian networks. *J. Hydrol.* **512**: 134–146, doi: 10.1016/j.jhydrol.2014.02.039.
Madadgar S, Moradkhani H. 2014b. Improved Bayesian multimodeling: integration of copulas and BMA. *Water Resour. Res.* **50**(12): 9586–9603, doi: 10.1002/2014WR015965.
Madhu S, Kumar TVL, Barbosa H, Rao KK, Bhaskar VV. 2015. Trend analysis of evapotranspiration and its response to droughts over India. *Theor. Appl. Climatol.* **121**(1-2): 41–51, doi: 10.1007/s00704-014-1210-3.
Makkonen L. 2008. Bringing closure to the plotting position controversy. *Commun. Stat. Theory Methods* **37**(3): 460–467.
Mao Y, Nijssen B, Lettenmaier DP. 2015. Is climate change implicated in the 2013-2014 California drought? A hydrologic perspective. *Geophys. Res. Lett.* **42**(8): 2805–2813, doi: 10.1002/2015GL063456.
Mavromatis T. 2007. Drought index evaluation for assessing future wheat production in Greece. *Int. J. Climatol.* **27**(7): 911–924.
McKee TB, Doeskin NJ, Kleist J. 1993. The relationship of drought frequency and duration to time scales. In: *Proceedings of the 8th Conference on Applied Climatology*, Anaheim, CA. American Meteorological Society: Boston, MA, 179–184.
Meque A, Abiodun BJ. 2015. Simulating the link between ENSO and summer drought in Southern Africa using regional climate models. *Clim. Dyn.* **44**(7-8): 1881–1900.
Mishra AK, Singh VP. 2010. A review of drought concepts. *J. Hydrol.* **391**(1-2): 202–216, doi: 10.1016/j.jhydrol.2010.07.012.
Najafi MR, Moradkhani H. 2015a. Multi-model ensemble analysis of runoff extremes for climate change impact assessments. *J. Hydrol.* **525**: 352–361, doi: 10.1016/j.jhydrol.2015.03.045.
Najafi MR, Moradkhani H. 2015b. Ensemble combination of seasonal streamflow forecasts. *J. Hydrol. Eng.* **21**(1): 4015043.
Nasrollahi N, AghaKouchak A, Cheng L, Damberg L, Phillips TJ, Miao C, Hsu K, Sorooshian S. 2015. How well do CMIP5 climate simulations replicate historical trends and patterns of meteorological droughts? *Water Resour. Res.* **51**(4): 2847–2864, doi: 10.1002/2014WR016318.
Orlowsky B, Seneviratne SI. 2013. Elusive drought: uncertainty in observed trends and short-and long-term CMIP5 projections. *Hydrol. Earth Syst. Sci.* **17**(5): 1765–1781.
Otkin JA, Anderson MC, Hain C, Svoboda M, Johnson D, Mueller R, Tadesse T, Wardlow B, Brown J. 2016. Assessing the evolution of soil moisture and vegetation conditions during the 2012 United States flash drought. *Agric. For. Meteorol.* **218**: 230–242.
Palmer WC. 1965. *Meteorological Drought*. US Department of Commerce, Weather Bureau: Washington, DC.
Park C-K, Byun H-R, Deo R, Lee B-R. 2014. Drought prediction till 2100 under RCP 8.5 climate change scenarios for Korea. *J. Hydrol.* **526**: 221–230, doi: 10.1016/j.jhydrol.2014.10.043.
Rana A, Moradkhani H. 2016. Spatial, temporal and frequency based climate change assessment in Columbia River Basin using multi downscaled-Scenarios. *Clim. Dyn.* **47**: 579–600.
Rana A, Moradkhani H, Qin Y. 2016. Understanding the joint behavior of temperature and precipitation for climate change impact studies. *Theor. Appl. Climatol.* doi:10.1007/s00704-016-1774-1
Risley J, Moradkhani H, Hay L, Markstrom S. 2011. Statistical comparisons of watershed-scale response to climate change in selected basins across the United States. *Earth Interact.* **15**(14): 1–26, doi: 10.1175/2010EI364.1.
Rupp DE, Abatzoglou JT, Hegewisch KC, Mote PW. 2013. Evaluation of CMIP5 20 th century climate simulations for the Pacific Northwest USA. *J. Geophys. Res. Atmos.* **118**(19): 10,884–10,906, doi: 10.1002/jgrd.50843.
Seager R, Tzanova A, Nakamura J. 2009. Drought in the southeastern United States: causes, variability over the last millennium, and the potential for future hydroclimate change*. *J. Clim.* **22**(19): 5021–5045.
Seager R, Hoerling M, Schubert S, Wang H, Lyon B, Kumar A, Nakamura J, Henderson N. 2015. Causes of the 2011–14 California drought*. *J. Clim.* **28**(18): 6997–7024, doi: 10.1175/JCLI-D-14-00860.1.
Sheffield J, Wood E. 2008. Projected changes in drought occurrence under future global warming from multi-model, multi-scenario, IPCC AR4 simulations. *Clim. Dyn.* **31**(1): 79–105.
Sheffield J, Wood EF, Roderick ML. 2012. Little change in global drought over the past 60 years. *Nature* **491**(7424): 435–438, doi: 10.1038/nature11575.
Sheffield J, Barrett AP, Colle B, Nelun Fernando D, Fu R, Geil KL, Hu Q, Kinter J, Kumar S, Langenbrunner B. 2013. North American climate in CMIP5 experiments. Part I: evaluation of historical simulations of continental and regional climatology*. *J. Clim.* **26**(23): 9209–9245.
Shukla S, Safeeq M, Aghakouchak A, Guan K, Funk C. 2015. Temperature impacts on the water year 2014 drought in California. *Geophys. Res. Lett.* **42**(11): 4384–4393, doi: 10.1002/2015GL063666.
Sima S, Ahmadalipour A, Tajrishy M. 2013. Mapping surface temperature in a hyper-saline lake and investigating the effect of temperature distribution on the lake evaporation. *Remote Sens. Environ.* **136**: 374–385.
Stagge JH, Tallaksen LM, Gudmundsson L, Van Loon AF, Stahl K. 2015. Candidate distributions for climatological drought indices (SPI and SPEI). *Int. J. Climatol.* **35**(13): 4027–4040, doi: 10.1002/joc.4267.
Strzepek K, Yohe G, Neumann J, Boehlert B. 2010. Characterizing changes in drought risk for the United States from climate change. *Environ. Res. Lett.* **5**(4): 044012, doi: 10.1088/1748-9326/5/4/044012.
Swain S, Hayhoe K. 2014. CMIP5 projected changes in spring and summer drought and wet conditions over North America. *Clim. Dyn.* **44**(9–10): 2737–2750, doi: 10.1007/s00382-014-2255-9.
Swain S, Hayhoe K. 2015. CMIP5 projected changes in spring and summer drought and wet conditions over North America. *Clim. Dyn.* **44**(9-10): 2737–2750, doi: 10.1007/s00382-014-2255-9.
Taylor KE, Stouffer RJ, Meehl G a. 2012. An overview of CMIP5 and the experiment design. *Bull. Am. Meteorol. Soc.* **93**(4): 485–498, doi: 10.1175/BAMS-D-11-00094.1.
Thober S, Kumar R, Sheffield J, Mai J, Schäfer D, Samaniego L. 2015. Seasonal soil moisture drought prediction over Europe using the North American Multi-Model Ensemble (NMME). *J. Hydrometeorol.* **16**(6): 2329–2344, doi: 10.1175/JHM-D-15-0053.1.
Thornthwaite CW. 1948. An approach toward a rational classification of climate. *Soil Sci.* **66**(1): 77, doi: 10.1097/00010694-194807000-00007.

Thrasher B, Maurer EP, McKellar C, Duffy PB. 2012. Technical note: bias correcting climate model simulated daily temperature extremes with quantile mapping. *Hydrol. Earth Syst. Sci.* **16**(9): 3309–3314, doi: 10.5194/hess-16-3309-2012.

Touma D, Ashfaq M, Nayak M a, Kao S-C, Diffenbaugh NS. 2015. A multi-model and multi-index evaluation of drought characteristics in the 21st century. *J. Hydrol.* **526**: 196–207, doi: 10.1016/j.jhydrol.2014.12.011.

Trenberth KE, Dai A, van der Schrier G, Jones PD, Barichivich J, Briffa KR, Sheffield J. 2014. Global warming and changes in drought. *Nat. Clim. Change* **4**(1): 17–22, doi: 10.1038/NCLIMATE2067.

Ujeneza EL, Abiodun BJ. 2015. Drought regimes in Southern Africa and how well GCMs simulate them. *Clim. Dyn.* **44**(5-6): 1595–1609.

Van Loon AF. 2015. Hydrological drought explained. *Wiley Interdiscip Rev Water* **2**(4): 359–392, doi: 10.1002/wat2.1085.

Vicente-Serrano SM, Beguería S, López-Moreno JI. 2010. A multiscalar drought index sensitive to global warming: the standardized precipitation evapotranspiration index. *J. Clim.* **23**(7): 1696–1718, doi: 10.1175/2009JCLI2909.1.

Weibull W. 1939. *A Statistical Theory of the Strength of Materials*. Generalstabens Litografiska Anstalts Förlag.

Werner AT. 2011. *BCSD Downscaled Transient Climate Projections for Eight Select GCMs over British Columbia, Canada*. Pacific Climate Impacts Consortium, University of Victoria: Victoria, BC, 63.

Williams AP, Seager R, Abatzoglou JT, Cook BI, Smerdon JE, Cook ER. 2015. Contribution of anthropogenic warming to California drought during 2012–2014. *Geophys. Res. Lett.* **42**: 6819–6828, doi: 10.1002/2015GL064924.

Willmott CJ, Robeson SM. 1995. Climatologically aided interpolation (CAI) of terrestrial air temperature. *Int. J. Climatol.* **15**(2): 221–229, doi: 10.1002/joc.3370150207.

Yu M, Li Q, Hayes MJ, Svoboda MD, Heim RR. 2014. Are droughts becoming more frequent or severe in China based on the standardized precipitation evapotranspiration index: 1951–2010? *Int. J. Climatol.* **34**(3): 545–558.

Zhao T, Dai A. 2015. The magnitude and causes of global drought changes in the twenty-first century under a low–moderate emissions scenario. *J. Clim.* **28**(11): 4490–4512.

